

Supernormal vision and high-resolution retinal imaging through adaptive optics

Junzhong Liang, David R. Williams, and Donald T. Miller*

Center for Visual Science, University of Rochester, Rochester, New York 14627

Received January 8, 1997; revised manuscript received May 12, 1997; accepted May 20, 1997

Even when corrected with the best spectacles or contact lenses, normal human eyes still suffer from monochromatic aberrations that blur vision when the pupil is large. We have successfully corrected these aberrations using adaptive optics, providing normal eyes with supernormal optical quality. Contrast sensitivity to fine spatial patterns was increased when observers viewed stimuli through adaptive optics. The eye's aberrations also limit the resolution of images of the retina, a limit that has existed since the invention of the ophthalmoscope. We have constructed a fundus camera equipped with adaptive optics that provides unprecedented resolution, allowing the imaging of microscopic structures the size of single cells in the living human retina. © 1997 Optical Society of America [S0740-3232(97)01111-3]

1. INTRODUCTION

It has long been known that the normal human eye suffers from many monochromatic aberrations that degrade retinal image quality. Helmholtz, commenting on the eye, put it as follows: "Now, it is not too much to say that if an optician wanted to sell me an instrument which had all these defects, I should think myself quite justified in blaming his carelessness in the strongest terms, and giving him back his instrument."¹ Although spectacles have been used to correct defocus since perhaps the thirteenth century^{2,3} and astigmatism since the nineteenth century,⁴ current ophthalmic lenses still leave uncorrected additional aberrations such as spherical aberration, coma, and a host of irregular aberrations. The pattern of aberrations left uncorrected by spectacles varies across individuals,⁵⁻⁹ and their combined effect reduces optical quality so that the eye's best optical performance occurs with a small pupil roughly 3 mm in diameter.

If the eye's aberrations could be completely corrected across a dilated pupil, significant improvement in the eye's optical quality would be expected, as illustrated in Fig. 1. It shows the large gap between the modulation transfer function (MTF) of human eyes with the optimum 3-mm pupil and the MTF of an aberration-free eye with an 8-mm pupil. Improving the optical quality of the eye will provide a new way to study neural limits on spatial vision that are otherwise confounded with the eye's optical blur. It may eventually lead to techniques to enhance visual performance beyond that provided by current spectacles and contact lenses. In addition, improving the eye's optical quality can improve the resolution of fundus images; such improvement could be valuable in basic studies of the living human retina as well as in clinical diagnosis and treatment of retinal pathology.

There have been various attempts to correct the eye's monochromatic aberrations beyond defocus and astigmatism. For viewing sinusoidal gratings in the laboratory, all aberrations of the eye can be avoided with interference fringes imaged on the retina.¹⁰⁻¹³ However, this tech-

nique is impractical for viewing stimuli other than gratings and is of no use for improving normal vision and the quality of fundus images. Another approach is to use a contact lens to null the refraction at the first surface of the cornea. This approach has the advantages of simplicity and low cost, but its effectiveness depends on the extent to which the corneal surface dominates in the combined effects of refractive-index variations throughout the eye's optics. When Thomas Young first discovered the astigmatism of the eye, he found that the astigmatism in his own eye remained essentially the same when he nulled the refraction at the cornea by immersing his eye in water.¹⁴ Possibly for this reason, a recent attempt to use a fundus contact lens to increase the axial resolution of a confocal laser scanning ophthalmoscope¹⁵ showed only modest improvement.

Adaptive optics could potentially correct for the total wave aberration of the eye and is well suited to cope with the large variation in the pattern of aberrations from eye to eye. Babcock originally proposed that adaptive optics could correct the dynamic wave-front error that atmospheric turbulence causes in ground-based telescopes,¹⁶ and this technique has been successfully implemented in astronomy.¹⁷⁻²⁰ Dreher *et al.* first used a deformable mirror in conjunction with the human eye.²¹ They succeeded in correcting the astigmatism in one subject's eye by using the prescription provided by a conventional refraction. The recent development of a Hartmann-Shack wave-front sensor for the eye⁸ has improved the measurement of the eye's aberrations.⁹ We have combined a Hartmann-Shack wave-front sensor with a deformable mirror to correct these aberrations and have applied this device to study both the visual performance and the retinal images of eyes corrected to provide supernormal image quality.

2. METHOD

Figure 2 shows the experimental setup, which consisted of an adaptive optics system combined with a system for

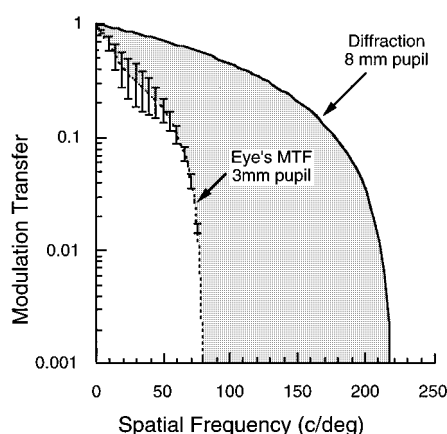


Fig. 1. Potential improvement in the eye's MTF by correction of the eye's high-order aberrations. Shown is the best MTF of the eye in normal viewing, obtained with a 3-mm pupil averaged across 14 eyes,⁹ with an optimal correction of defocus and astigmatism, and the ideal MTF of the eye for an 8-mm pupil blurred only by diffraction. The shaded region shows the range of contrasts and spatial frequencies that are inaccessible both for the case of imaging patterns on the retina and for the case of imaging the retina outside the eye.

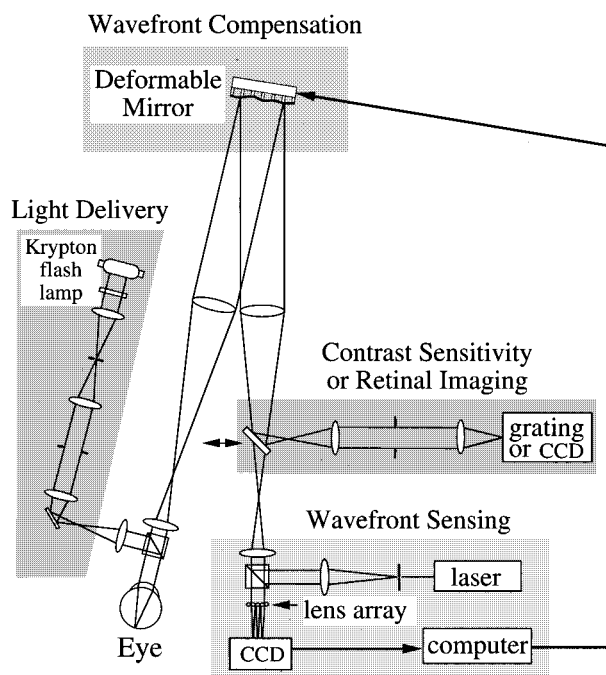


Fig. 2. Optical system. *Wavefront sensing and adaptive compensation.* The eye focused a collimated laser beam onto the retina. The light reflected from the retina formed an aberrated wave front at the pupil. The distorted wave front is measured by a Hartmann–Shack wave-front sensor. A deformable mirror, conjugate with the pupil, compensated for the eye's wave aberration. After compensation was achieved, psychophysical or retinal imaging experiments were performed with a 6-mm pupil. *Observations of point sources.* The point source from the wave-front sensor, attenuated to $\sim 8 \times$ detection threshold, was fixated through the compensated optics. *Contrast sensitivity.* A square-wave grating was viewed by insertion of a mirror in the path. Contrast sensitivity was measured with the method of adjustment by diluting contrast with a uniform background at constant retinal illuminance. *Retinal imaging.* A krypton flash lamp delivered a 4-ms flash, illuminating a retinal disk 1 deg in diameter. A scientific-grade CCD acquired images of the retina. Retinal location was controlled with a fixation target.

visual psychophysics and retinal imaging. The adaptive optics system contained a wave-front sensor, which measured the eye's wave aberration, and a deformable mirror, which corrected the wave aberration.

A. Wave-Front Sensing

We used a Hartmann–Shack wave-front sensor described in detail in Ref. 9. The eye focused a laser beam (He–Ne, 633-nm, 1.5-mm diameter at the eye's pupil) onto the retina. The visual angle subtended by the spot on the retina was 0.31 arc min. The light reflected from the retina formed a distorted wave front at the pupil, which was dilated with tropicamide (1%). A hexagonal array of 217 lenslets was conjugate with the eye's pupil plane. Each lenslet had a focal length of 97 mm and a diameter of 0.5 mm. The eye's pupil plane was magnified by 1.25 at the plane of the lenslet array, which sampled the wave front at the pupil with a center-to-center spacing of 0.4 mm across the central 6.76 mm of the pupil. Each lenslet formed an image of the light spot on the retina on a cooled, scientific-grade CCD array with 512×512 pixels. The displacement of each image on the CCD gave the local wave-front slope. From the array of slopes, the wave front was reconstructed with a least-squares technique^{8,22} with 65 Zernike modes.

B. Wave-Front Compensation

A deformable mirror (Xinetics, Inc.) compensated for the eye's wave aberration. The mirror consisted of an aluminized glass face plate with 37 lead zirconate-lead titanate (PZT) actuators mounted in a square array on the back surface. The stroke of the mirror beneath each actuator was $\pm 2 \mu\text{m}$, allowing a wave-front shift of $8 \mu\text{m}$ in the reflected beam. The full range of motion of each actuator was divided into 4096 steps (12 bits). The mirror lay in a plane conjugate with both the eye's pupil plane and the lenslet array of the wave-front sensor. The geometry of these three conjugate planes is shown in Fig. 3. The spacing of adjacent actuators on the mirror was 7 mm. The eye's pupil plane was magnified 6.25 times at the deformable mirror, so that the actuator spacing in the pupil plane was 1.12 mm. The high sampling density of the wave-front sensor was chosen to capture most of the higher-order aberrations in the eye's wave aberration, even though the mirror could not have compensated for all of them.

The observer's head position was secured with a bite bar. The observer aligned the center of his dilated pupil with respect to the axis of the instrument as follows. The observer adjusted his horizontal position until the left side of the pupil occluded his view of the laser point source that he was fixating. He repeated this task using the right side, the top, and the lower margin of the pupil. The average of two settings in each of these four locations was used to obtain the center of the entrance pupil.

Compensation was achieved with closed-loop feedback control. In each loop, six images, each of 300-ms duration and separated by 400 ms, were obtained with the wave-front sensor. The wave aberration in the system including the eye and mirror was computed from the sum of the six images and was evaluated at the locations of the actuators. In each loop we updated the actuators by cor-

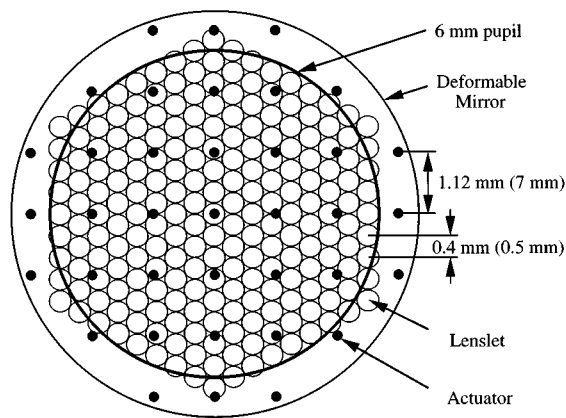


Fig. 3. Geometry of the 217 lenslets of the Hartmann-Shack wave-front sensor (open circles) and the location of the 37 actuators (filled circles) of the deformable mirror. The lenslet array and the mirror are shown imaged in the entrance pupil of the eye. The numbers in parentheses indicate the physical spacing of the actuators and the lenslets.

recting 10% of the error measured by the wave-front sensor. The value of 10% was chosen empirically because it caused well-behaved convergence on a minimum RMS wave-front error. Loops were repeated until the RMS wave-front error could be reduced no further, which usually required 10–20 loops. The improvement in the optical quality of the eye provided by the deformable mirror was evaluated in three ways: by computing the MTF and the point-spread function (PSF) from the wave-front sensor's measurements of the wave aberration, by measuring the observer's contrast sensitivity for gratings viewed through the deformable mirror, and by examining the quality of the images of the living retina taken through the deformable mirror. All experimental measurements used a 6-mm artificial pupil conjugate with the entrance pupil of the eye. The psychophysical and the retinal imaging experiments were performed by sliding a mirror into the path between the wave-front sensor and the deformable mirror (see Fig. 2).

C. Calculating the Optical Quality of the Eye

The wave aberration computed from the wave-front sensor provided the data from which the optical quality of the eye could be assessed. The pupil function is the product of the pupil transmittance function and the exponential of the wave aberration. The autocorrelation of the pupil function was taken as the MTF of the eye.²³ The pupil transmittance function was assumed to be uniform. No correction was made for the Stiles-Crawford effect,^{24,25} as we have found its effect on the MTF to be small even for this relatively large pupil size. The squared modulus of the Fourier transform of the pupil function gave the PSF of the eye.

D. Measuring Contrast Sensitivity

The eye's astigmatism was corrected with trial lenses selected by the observer to optimize the subjective image quality of a pattern of white dots on a black background. The eye's defocus was then reduced by asking the observer to translate the lens in front of his eye in tandem with his eye along the optical axis, to maximize the ap-

parent contrast of a horizontal grating at 27.5 c/deg with the mirror flat. The square-wave gratings were placed in the same plane as the dot pattern that had been used to correct astigmatism. The grating stimulus was produced by backilluminating with tungsten light a sandwich composed of a diffuser, a 630-nm interference filter, and a horizontal Ronchi ruling. A second channel provided a uniform background at the same wavelength, which was used to dilute the grating contrast. Each channel contained a linear polarizer at right angles to each other. An analyzer in the common path allowed the contrast to be adjusted at a constant retinal illuminance of 900 td. Gratings were steadily presented in a field subtending 0.6 deg. Contrast sensitivity was measured with the method of adjustment at two spatial frequencies, 27.5 and 55 c/deg for two observers before and after adaptive compensation. Approximately 15 measurements were made at each spatial frequency by each observer.

E. Imaging the Retina

The observer fixated a crosshair which determined the retinal location to be imaged. When the subject was ready, a krypton flash lamp delivered a 4-ms flash, illuminating a retinal disk 1 deg in diameter. The short 4-ms exposure helped to prevent motion blur resulting from the movement of the retina during each exposure. The lamp output, which was broadband white light, was filtered with a 10-nm-bandwidth interference filter centered at 630 nm. The retinal irradiance of the flash was 5.7 mW/mm², which is approximately 90 times less than the American National Standards Institute's maximum permissible exposure for this retinal image size.²⁶ To produce images of the retina, a scientific-grade CCD was positioned conjugate with the retina, in the plane that previously contained the grating stimuli used in the psychophysical experiments. Each CCD pixel subtended 8 arc sec, corresponding to a sampling frequency at the retina of 450 c/deg. Images were acquired when the mirror was flat (uncompensated imaging) and when the mirror was warped to correct the eye's wave aberration (compensated imaging). For both the compensated and the uncompensated imaging, astigmatism was corrected with trial lenses by using the amount of astigmatism measured with the wave-front sensor when the mirror was flat. For uncompensated imaging, the optimum focus was determined by translating in tandem the eye and the lens nearest the eye to achieve the highest-contrast retinal images. For compensated imaging, the optimum focus was provided directly by the wave-front sensor and the mirror, and further refocusing usually did not improve the quality of the retinal images.

3. RESULTS

A. Optical Quality of the Eye

Figure 4 shows the wave aberration for two subjects (JL and DM) before and after adaptive compensation. Though still not completely planar, the wave front after compensation is much flatter. In the four subjects measured, adaptive compensation reduced the peak-to-valley wave-front error across a 6-mm pupil by a factor of 4 on average.

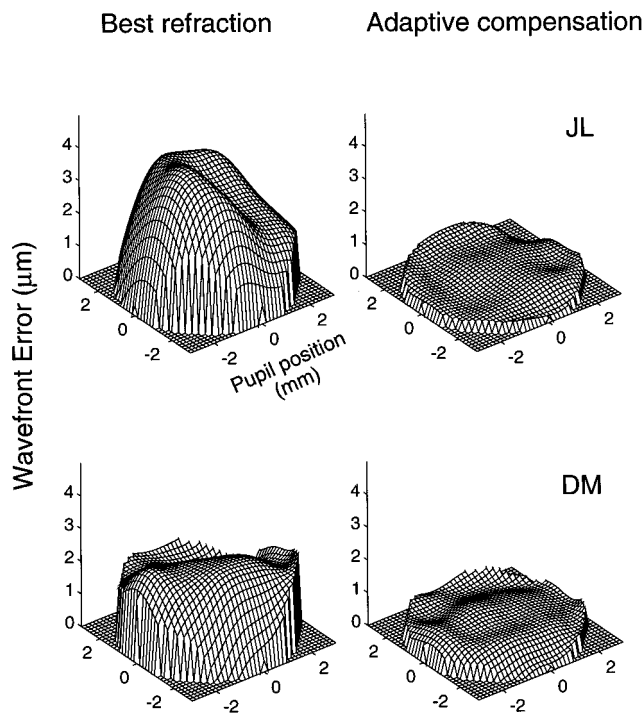


Fig. 4. Wave aberration for two eyes (JL and DM) without and with adaptive compensation for a 6-mm pupil. For the uncompensated case, trial lenses were used to correct the astigmatism. According to the wave-front-sensor measurements, the astigmatism left uncorrected by the trial lenses is 0.28 D and 0.27 D for JL and DM, respectively. Defocus of the eye was corrected with trial lenses so that the highest-contrast images of the retina were obtained when the deformable mirror was flat.

To determine which aberrations were corrected by the deformable mirror, we decomposed the wave aberration of the eye into 65 Zernike modes up to tenth order (see Ref. 9 for details). Figure 5 compares the measured RMS wave-front error of each Zernike order for the eyes without adaptive compensation with the error after adaptive compensation. The lower Zernike orders up to fourth order were significantly reduced, while aberrations beyond sixth order remain almost unchanged.

The second-order Zernike aberrations are defocus and astigmatism. The mean value of the astigmatism in the four eyes left uncorrected by trial lenses was ~ 0.2 diopters (D). The mean defocus in the second-order Zernike mode was ~ 0.4 D. Although, it would appear that the eyes were not well refracted with trial lenses in the uncompensated case, the existence of high-order aberrations often requires some defocus for the best optical quality to be achieved.

Our results show that with adaptive compensation we can correct not only the eye's defocus and astigmatism but also coma, spherical aberration, and other irregular aberrations in the eye. By increasing the number of actuators of the deformable mirror, one could also presumably correct still-higher-order irregular aberrations in the eye.

Figure 6 shows the PSF's for the two subjects whose wave aberrations are shown in Fig. 4. The eye's PSF's before adaptive compensation have multiple peaks that are due to coma and irregular aberrations in the eye. For the best correction that is shown here for these two eyes, adaptive compensation increased the Strehl ratio from

0.05 to 0.47 for subject JL and from 0.05 to 0.33 for subject DM. After compensation, the PSF for both JL and DM has a full width at half-height (FWHH) of $2.0 \mu\text{m}$, close to the value of $1.9 \mu\text{m}$ expected from diffraction alone. This is smaller than the diameter of a foveal cone and is ~ 2.0 times narrower than the FWHH obtained with a diffraction-limited 3.0-mm pupil, the pupil size that gives about the best image quality in normal viewing.

Figure 7 shows the MTF, averaged across all orientations, for JL and DM as well as the MTF limited only by

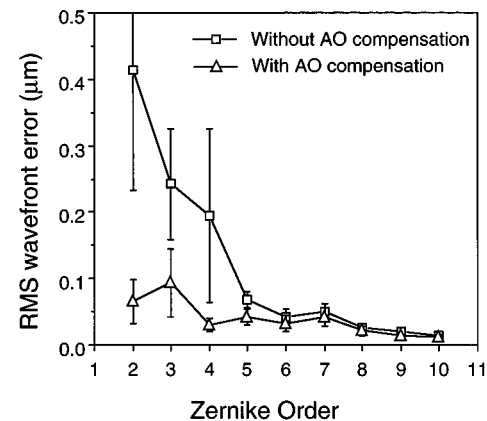


Fig. 5. RMS wave-front error of the eye before and after compensation with adaptive optics (AO). The result is averaged from measurements for four subjects. The abscissa is the Zernike order of the Zernike expansion.⁹ The second-order Zernike aberrations are for defocus and astigmatism, the third-order for coma and comalike aberrations, and the fourth-order for spherical and other aberrations. The higher-order (beyond fourth-order) modes are irregular aberrations.

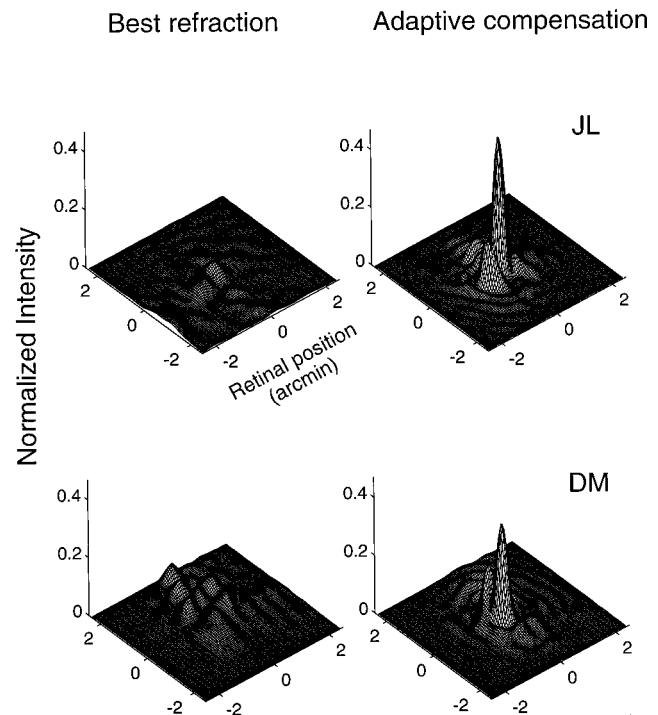


Fig. 6. PSF of the eye for subjects JL and DM without and with adaptive compensation for a 6-mm pupil. The PSF's were computed from the corresponding wave aberrations shown in Fig. 4.

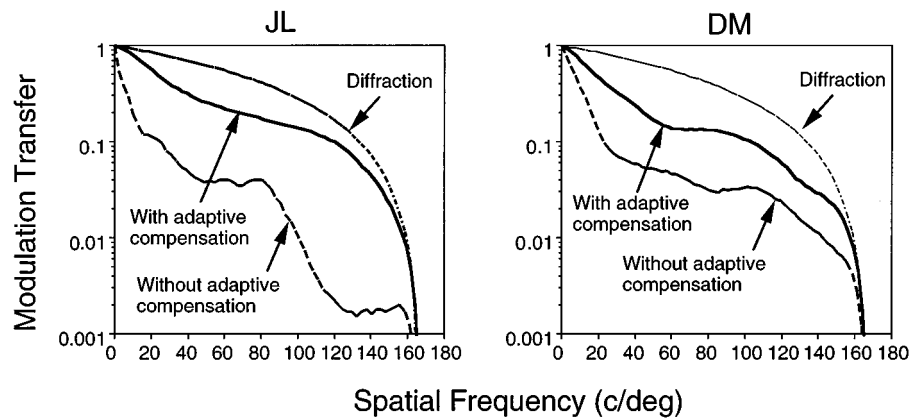


Fig. 7. Eye's radially averaged modulation transfer function for subjects JL and DM without and with adaptive compensation for a 6-mm pupil. The eye's MTF's were calculated from the wave aberrations shown in Fig. 4.

diffraction for the same pupil size, 6 mm. Although it is still lower than the MTF limited only by diffraction for the 6-mm pupil, the eye's MTF with adaptive compensation is significantly higher than that obtained without compensation.

Figure 8 shows the mean of the radially averaged MTF for the four eyes measured before and after adaptive compensation for a 6-mm pupil, plus the mean of the radially averaged MTF of the same four eyes for a 3-mm pupil without adaptive compensation. The MTF at 3 mm exemplifies the best MTF in normal viewing. Adaptive compensation provided the eye with the best MTF at all spatial frequencies, the benefit increasing with increasing spatial frequency until near the resolution limit set by diffraction.

B. Contrast Sensitivity

Figure 9 shows contrast-sensitivity measurements for two observers before and after adaptive compensation. Filled symbols show contrast sensitivity without adaptive compensation, i.e., with the deformable mirror flat. Open symbols show the contrast sensitivity when the mirror corrects the eye's aberrations. At 55 c/deg, neither observer could detect the grating when the deformable mirror was flat, even at 100% contrast. This was true no matter what pupil size we tried and despite attempts to correct defocus and astigmatism with trial lenses. With adaptive compensation, the observers required approximately 40% contrast on average to detect the grating. At another spatial frequency, 27.5 c/deg, contrast sensitivity was improved by close to a factor of 6 by adaptive compensation. Contrast-sensitivity measurements have been made on observer DRW under a variety of conditions over a number of years. The contrast sensitivity reported here with adaptive optics is higher than any previous measurements on his eye, including those obtained with a 3-mm pupil and optimized refraction, with the exception of measurements made with interference fringes. These preliminary psychophysical results provide additional evidence that the eye's optical performance is improved by adaptive compensation.

C. Images of the Retina

Recently techniques have succeeded in recovering very-high-spatial-frequency information from the living hu-

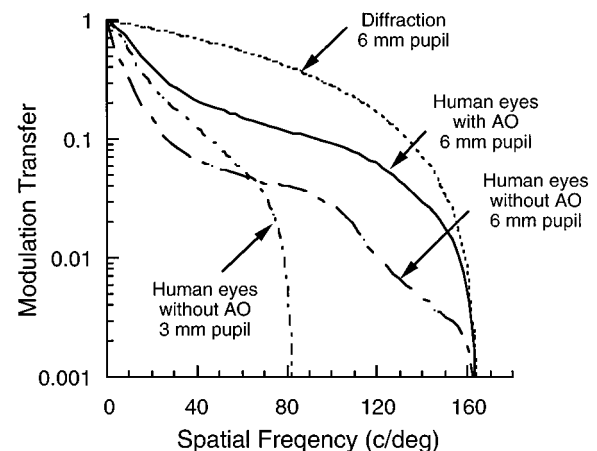


Fig. 8. Mean MTF's of the four tested eyes before and after adaptive compensation, together with the eye's MTF for a 3-mm pupil, which is presumably the best MTF with a conventional correction. The MTF's were derived from the truncated wave aberration measured with the wave-front sensor within a 6.76-mm pupil.

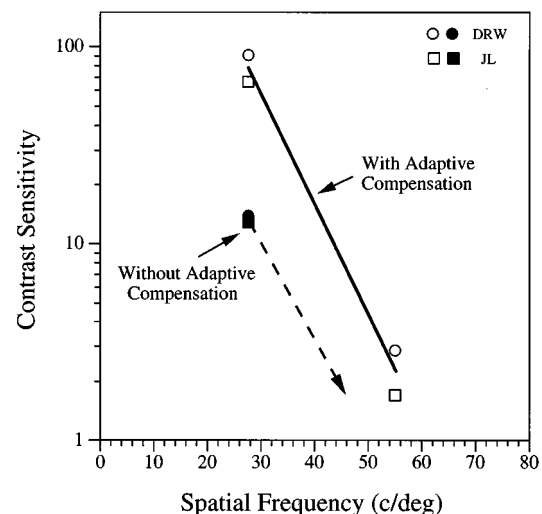


Fig. 9. Contrast-sensitivity measurement for two eyes (JL and DRW) for a horizontal grating of 27.5 and 55 c/deg with and without adaptive compensation.

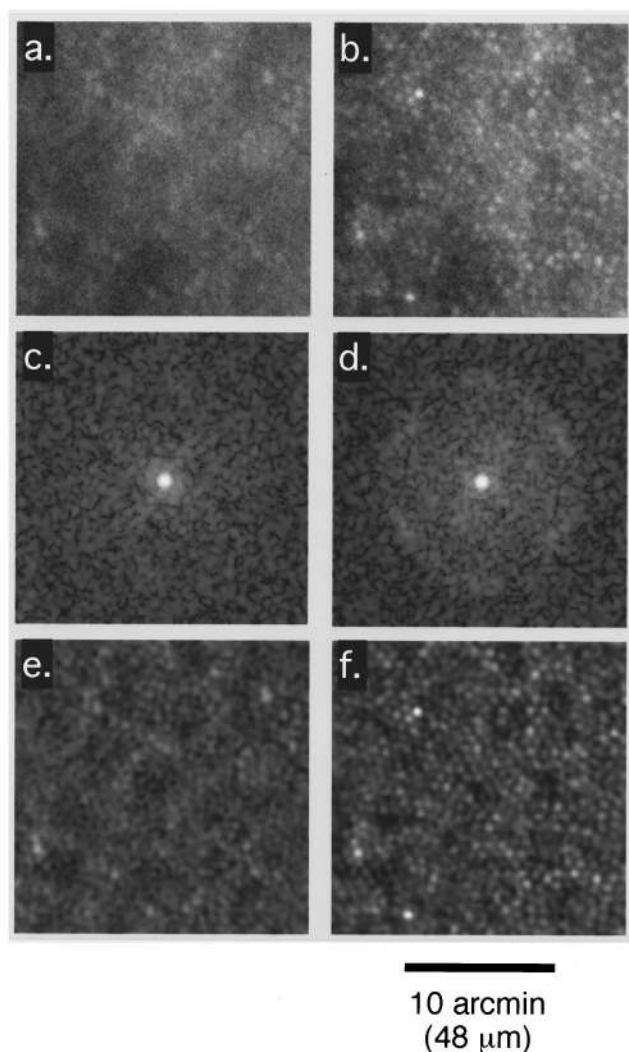


Fig. 10. Image from DM's retina at 0.8-deg eccentricity without (a.) and with (b.) adaptive compensation for a 6-mm pupil. Each image is a 20-arc-min square or approximately $96 \times 96 \mu\text{m}^2$ at the retina. The power spectra of the images in a. and b. are shown in c. and d., respectively. In the compensated power spectrum in d., the ring of power at $\sim 86 \text{ c/deg}$ indicates the sampling frequency of the photoreceptors at this retinal location. e. and f. show bandpass-filtered images without and with compensation, respectively. A Butterworth filter, chosen to remove high-spatial-frequency noise and to enhance contrast, passed frequencies between 0.1 and 1.2 times the sampling frequency of cones determined from the power spectrum. For comparative purposes, the contrast ratio between the two filtered images was set to that of the original images in a. and b.

man retina. Estimates of the dimensions of microscopic structures in living human retinas have been obtained with coherent²⁷ and incoherent²⁸ light under conditions in which only defocus and astigmatism in the eye were corrected. Cone spacing of living retinas can be estimated on the basis of the power spectra of retinal images in coherent light, but laser speckle associated with coherent imaging and imaging blur that is due to the eye's aberrations prevent the resolution of these retinal structures in single exposures. Miller *et al.*²⁸ showed, using incoherent light, that when defocus and astigmatism are carefully corrected, the cone mosaic can sometimes be re-

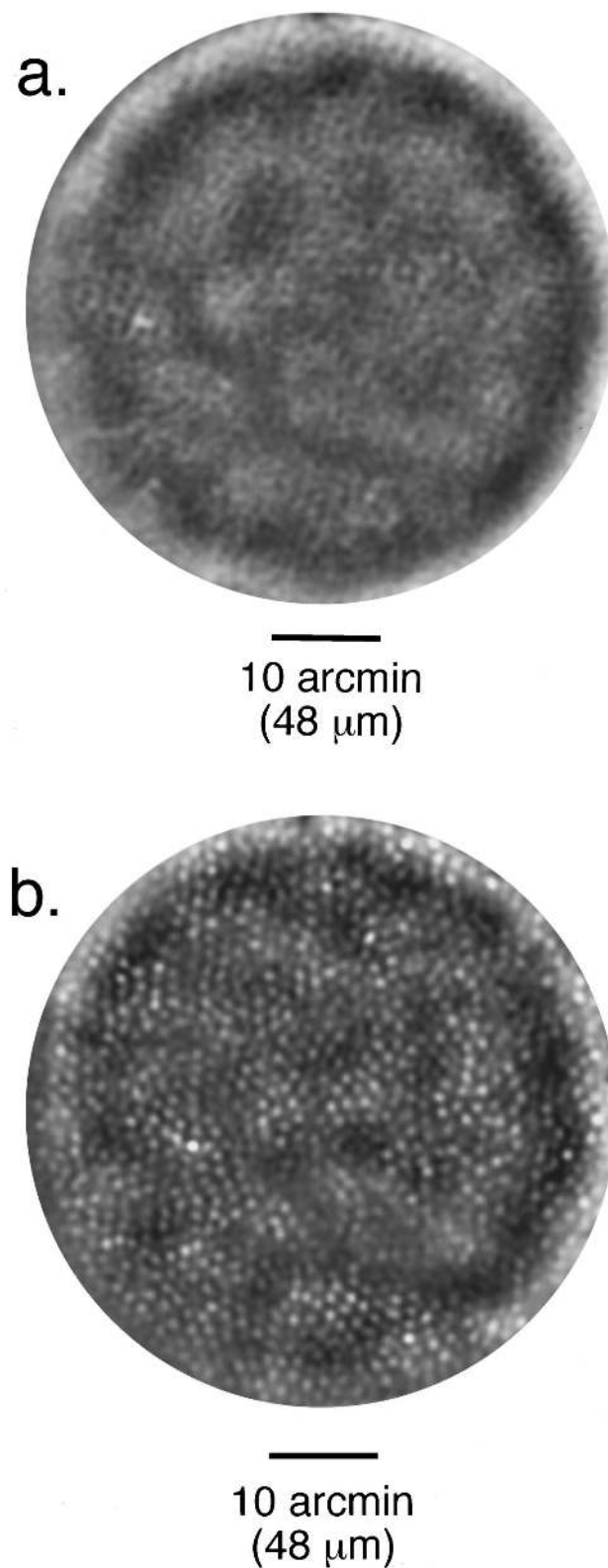


Fig. 11. Image of the retina at 4-deg eccentricity for subject DM without adaptive compensation (a.) and with adaptive compensation (b.) Each image subtends $\sim 1 \text{ deg}$ or $291 \mu\text{m}$ at the retina. From the power spectrum of the compensated image, the mean sampling frequency was estimated at 46 c/deg . The images shown have been bandpass filtered, passing frequencies from 5 to 60 c/deg .

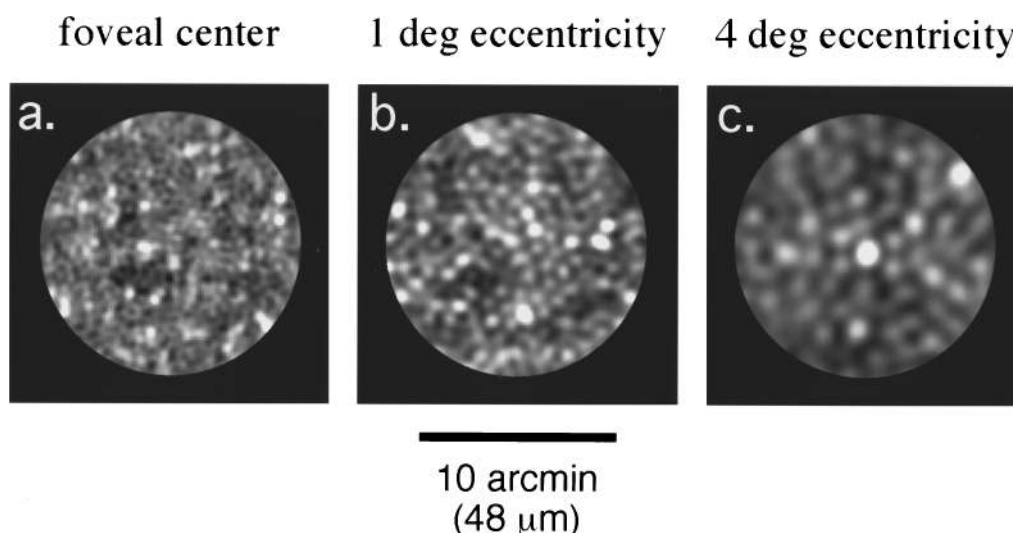


Fig. 12. Images of the cone mosaic from subject JL's eye obtained with adaptive compensation at the foveal center (a.), at 1-deg eccentricity (b.), and at 4-deg eccentricity (c.) in the temporal retina, showing the decline in cone density with retinal eccentricity. Each image subtends 13.3 arc min or $64\ \mu\text{m}$ at the retina. The images have been bandpass filtered as in Fig. 3. The sampling frequencies were 110, 73, and 46 c/deg for 0, 1, and 4 deg, respectively, corresponding to row spacings of 2.6, 3.9, and $6.3\ \mu\text{m}$. Similar data were obtained for DM, whose row spacings were 2.6, 3.4, and $6.4\ \mu\text{m}$ for 0, 1, and 4 deg, respectively.

solved in individual retinal images, though only at a narrow range of retinal eccentricities in a few eyes that had exceptional optical quality. In the best subject in that study (JL), we were not able to resolve cones at the foveal center or at eccentricities greater than 2.5 deg, nor was it possible to resolve cones in any individual image for DM's eye without adaptive optics. When the optical quality of the eye was improved with adaptive optics, we were consistently able to resolve individual cones at all retinal locations imaged in all five subjects to date. This includes imaging cones from the foveal center to 4-deg eccentricity for two subjects (DM and JL).

Figures 10a. and 10b. show images of the same retinal location (0.8-deg eccentricity) for subject DM, without and with adaptive compensation, respectively. The image with adaptive compensation shows more structure and has higher contrast. The power spectrum of the image obtained with adaptive compensation, shown in Fig. 10d., contains power in a ring of spatial frequencies, the signature of the cone mosaic first described in spectra of anatomical sections by Yellott.²⁹ This ring is not evident in the power spectrum of the image obtained without compensation, shown in Fig. 10c. Figures 10e. and 10f. show the same retinal images following bandpass filtering to increase contrast and remove high-spatial-frequency noise.

Figures 11a. and 11b. show 1-deg images of DM's retina at 4-deg eccentricity before and after adaptive compensation, respectively. With adaptive compensation, cones within the 1-deg field can be clearly resolved, whereas it is difficult to resolve cones in the uncompensated image, even though the size of the cones is as large as $6.3\ \mu\text{m}$ (46 c/deg) in this retinal eccentricity. In these images, as well as those obtained at other retinal locations, there is no evidence of a variation in image quality across the image. This indicates that the isoplanatic patch, which limits the compensated field of view to only a few arcseconds for ground-based telescopes,³⁰ is at least as large as the 1-deg field of our present instrument.

Figure 12 shows cones from the foveal center to 4-deg eccentricity for subject JL with adaptive compensation for his eye's wave aberration. The variation in the intensity of different spots in these images is a consistent feature. Repeated exposures of the same retinal patch show the same pattern. The cause of these variations is not known. Adaptive optics allowed us to resolve cones over the same range of eccentricities in subject DM, even though we were unable to resolve cones in any individual image for his eye without adaptive optics.²⁸ The cone spacing and packing arrangement, accessible here in living retina, is similar to that obtained in anatomical studies of excised retinas.³¹

4. DISCUSSION

Three sources of evidence show that adaptive optics provide what is probably the best optical quality ever achieved in the human eye: estimates of the eye's MTF and PSF from wave-front sensing, psychophysical measurements of contrast sensitivity, and the improved quality of images of the retina. By using monochromatic light, we avoided the eye's chromatic aberration. For the presentation of broadband visual stimuli or for retinal imaging in color through adaptive optics, axial chromatic aberration could be corrected with an achromatizing lens.³²

A. Visual Benefit of Adaptive Optics

When the pupil is large, correcting the high-order aberrations of the normal eye provides additional improvement in the eye's optical quality beyond a conventional correction of only defocus and astigmatism. In bright daylight conditions, the natural pupil of most normal eyes is sufficiently small ($\sim 3\ \text{mm}$) that diffraction dominates and monochromatic aberrations beyond defocus and astigmatism are negligible. However, correction of high-order aberrations with a device such as a deformable mirror, or perhaps eventually with a custom contact lens, would provide the greatest visual benefit when the pupil is large or

for eyes that have high amounts of aberrations beyond defocus and astigmatism. The compact PSF with adaptive compensation makes it possible for the eye to take full advantage of a large pupil, thereby improving the efficiency for collecting more photons and increasing the capability to resolve finer details as well. We have shown that eyes with adaptive compensation can resolve fine gratings (55 c/deg) that were invisible under normal viewing conditions. For lower-spatial-frequency gratings that were visible without adaptive optics, the contrast sensitivity was significantly increased after adaptive compensation. Stimuli such as edges viewed through the compensating deformable mirror have a strikingly crisp appearance consistent with the supernormal quality of the retinal image.

B. Exploration of Neural Limits on Vision

This preliminary evidence that the eye's visual performance is improved with the correction of additional high-order aberrations is encouraging for the further exploration of better vision for normal human eyes. If the optics of the eye were completely corrected, neural factors would set an upper bound for visual performance. It has been argued that evolution has optimized the human eye, giving it an optical quality that exceeds the grain of the retina.³³ Adaptive optics is a new tool to examine this theory and to investigate to what extent observers can take advantage of better retinal image quality than the eye has experienced before.

Neural limits on spatial vision can be explored with interferometry,¹⁰⁻¹³ which can produce unity contrast gratings on the retina that are not blurred by either aberrations or diffraction. Although adaptive optics can provide a large increase in retinal image contrast for high spatial frequencies viewed by the normal eye, stimuli imaged on the retina with incoherent light will still be blurred by diffraction at the pupil. However, adaptive optics has the distinct advantage that any visual stimulus, not just sinusoidal gratings, can be viewed at supernormal retinal image contrast. For example, observers JL and DW viewed a steady, 633-nm point source of approximately eight times detection threshold through the deformable mirror. The point source appeared sometimes green and sometimes red. The color fluctuation was much more robust with adaptive compensation than without. This effect, which is an example of chromatic aliasing,³⁴ has been attributed to the selective excitation of different cone classes as eye movements shift the retinal location illuminated by the point source.^{35,36} With adaptive compensation, the FWHH of the eye's PSF is often smaller than the diameter of a single foveal cone, increasing the fraction of time that only a single receptor is stimulated. Presumably, had we measured color discrimination under these conditions, it would have been impaired. The expectation is that improving the optics of the eye can actually cause visual performance to decline. Performance may also decline for certain other fine foveal tasks, such as two-dot vernier acuity.³⁷

C. Retinal Imaging

Adaptive optics also provides a noninvasive technique for studying the normal and the pathological living retina at a microscopic spatial scale. Our new fundus camera

equipped with adaptive optics provides unprecedented transverse resolution, so that the living retina can be seen at a spatial scale previously accessible only in excised retina. By correcting the eye's wave aberration for a 6-mm pupil, the PSF measurements suggest that the present system has created an eightfold increase in the Strehl ratio. This corresponds to about a twofold decrease in PSF FWHH over that obtained with a 3-mm pupil. The use of a larger pupil, shorter wavelengths, and a more sophisticated compensation device than our present 37-actuator mirror could further improve the optical quality of the eye. For fundus imaging, imperfect (partial) adaptive compensation may be further improved by post-processing techniques such as inverse filtering and phase diversity.^{38,39} Image restoration techniques applied after blurring by aberrations has occurred tend to be sensitive to noise, whereas adaptive optics precludes blurring to begin with. For this reason, it is unlikely that image restoration alone could provide the high-resolution images that are available from the use of adaptive optics.

If 555-nm illumination and an 8-mm pupil were used, one could in principle produce a FWHH of the PSF of 1.18 μm and a 3.2-fold increase in transverse resolution over that for a 2.5-mm pupil, a typical pupil diameter for current fundus cameras. The axial resolution, which is critical in optical sectioning of the retina in depth, grows as the square of the pupil diameter.^{21,40} Therefore complete adaptive compensation across an 8-mm pupil could theoretically increase the axial resolution of a confocal scanning laser ophthalmoscope by a factor of 10 over an instrument with a 2.5-mm exit pupil. The FWHH of the PSF in depth would be $\sim 30 \mu\text{m}$, approaching that of optical coherence tomography^{41,42} but providing the additional advantage of high transverse resolution and faster image acquisition.

ACKNOWLEDGMENTS

This research was supported by National Institutes of Health grants EY04367 and EY01319, a Rochester Eye and Human Parts Bank Fellowship, and an ophthalmology development grant from Research to Prevent Blindness, Inc. The authors are thankful to G. Michael Morris, A. Russell, H. Tamaddon, and W. Vaughn of the University of Rochester and to R. Fugate of Starfire Optical Range, Phillips Laboratory/LTE, for their technical assistance.

*Present address: Wright Laboratory, AAJT, Electro-Optics Sensor Technology Branch, Wright-Patterson Air Force Base, Ohio, 45433-7700.

REFERENCES

1. H. von Helmholtz, *Popular Scientific Lectures*, M. Kline, ed. (Dover, New York, 1962).
2. G. T. Cashell, "A short history of spectacles," *Proc. R. Soc. Med.* **64**, 1063-1064 (1971).
3. M. L. Rubin, "Spectacles: past, present and future," *Surv. Ophthalmol.* **30**, 321-327 (1986).
4. H. von Helmholtz, *Helmholtz's Treatise on Physiological Optics*, J. P. C. Southall, ed. (Optical Society of America, New York, 1924).
5. M. S. Smirnov, "Measurement of the wave aberration of the human eye," *Biophys. J.* **7**, 766-795 (1962).

6. H. C. Howland and B. Howland, "A subjective method for the measurement of monochromatic aberrations of the eye," *J. Opt. Soc. Am.* **67**, 1508–1518 (1977).
7. G. Walsh, W. N. Charman, and H. C. Howland, "Objective technique for the determination of monochromatic aberrations of the human eye," *J. Opt. Soc. Am. A* **1**, 987–992 (1984).
8. J. Liang, B. Grimm, S. Goelz, and J. Bille, "Objective measurement of the wave aberrations of the human eye with the use of a Hartmann–Shack wave-front sensor," *J. Opt. Soc. Am. A* **11**, 1949–1957 (1994).
9. J. Liang and D. R. Williams, "Aberrations and retinal image quality of the normal human eye," *J. Opt. Soc. Am. A* **14**, 2873–2883 (1997).
10. Y. L. Grand, "Sur la mesure de l'acuité visuelle au moyen de franges d'interférence," *Acad. Sci.* **200**, 490–491 (1935).
11. G. Westheimer, "Modulation thresholds for sinusoidal light distributions on the retina," *J. Physiol. (London)* **152**, 67–74 (1960).
12. F. W. Campbell and D. G. Green, "Optical and retinal factors affecting visual resolution," *J. Physiol. (London)* **181**, 576–593 (1965).
13. D. R. Williams, "Aliasing in human foveal vision," *Vision Res.* **25**, 195–205 (1985).
14. T. Young, "On the mechanism of the eye," *Philos. Trans. R. Soc. London* **91**, 23–88 (1801).
15. D. Bartsch, G. Zinser, and W. R. Freeman, "Resolution improvement of confocal scanning laser tomography of the human fundus," *Vision Science and Its Applications*, Vol. 2 of 1994 OSA Technical Digest Series (Optical Society of America, Washington, D.C., 1994), pp. 134–137.
16. H. W. Babcock, "The possibility of compensating astronomical seeing," *Publ. Astron. Soc. Pac.* **65**, 229–236 (1953).
17. J. W. Hardy, "Active optics: a new technology for the control of light," *Proc. IEEE* **66**, 651–697 (1978).
18. R. Q. Fugate, D. L. Fried, G. A. Ameer, B. R. Boeke, S. L. Browne, P. H. Roberts, R. E. Ruane, G. A. Tyler, and L. M. Wopat, "Measurement of atmospheric wavefront distortion using scattered light from a laser guide-star," *Nature* **352**, 144–146 (1991).
19. F. Merkle, in *International Trends in Optics*, J. Goodman, ed. (Academic, San Diego, Calif., 1991).
20. R. K. Tyson, *Principles of Adaptive Optics* (Academic, San Diego, Calif., 1991).
21. A. W. Dreher, J. F. Bille, and R. N. Weinreb, "Active optical depth resolution improvement of the laser tomographic scanner," *Appl. Opt.* **24**, 804–808 (1989).
22. W. H. Southwell, "Wave-front estimation from wave-front slope measurements," *J. Opt. Soc. Am.* **70**, 998–1006 (1980).
23. J. W. Goodman, *Introduction to Fourier Optics* (McGraw-Hill, San Francisco, Calif., 1968).
24. W. S. Stiles and B. H. Crawford, "The luminous efficiency of rays entering the eye pupil at different points," *Proc. R. Soc. London Ser. B* **112**, 428–450 (1933).
25. J. Enoch and V. Lakshminarayanan, "Retinal fibre optics," in *Visual Optics and Instrumentation*, W. N. Charman, ed., Vol. 1 of Vision and Visual Dysfunction, J. Cronly-Dillon, ed. (CRC, Boca Raton, Fla., 1991), Chap. 12.
26. American National Standards Institute, *American National Standard for the Safe Use of Lasers*, ANSI Z136.1-1993 (Laser Institute of America, Orlando, Fla., 1993).
27. S. Marcos, R. Navarro, and P. Artal, "Coherent imaging of the cone mosaic in the living human eye," *J. Opt. Soc. Am. A* **13**, 897–905 (1996).
28. D. T. Miller, D. R. Williams, G. M. Morris, and J. Liang, "Images of the cone mosaic in the living human eye," *Vision Res.* **36**, 1067–1079 (1996).
29. J. I. Yellott, Jr., "Spectral analysis of spatial sampling by photoreceptors: topological disorder prevents aliasing," *Vision Res.* **22**, 1205–1210 (1982).
30. J. Hardy, "Instrumental limitation in adaptive optics for astronomy," in *Active Telescope Systems*, F. J. Roddier, ed., Proc. SPIE **1114**, 2–13 (1989).
31. C. A. Curcio, K. R. Sloan, R. E. Kalina, and A. E. Hendrickson, "Human photoreceptor topography," *J. Comp. Neurol.* **292**, 497–523 (1990).
32. R. E. Bedford and G. W. Wyszecki, "Axial chromatic aberration of the human eye," *J. Opt. Soc. Am.* **47**, 564–565 (1957).
33. A. W. Snyder, T. R. J. Bossomaier, and A. Hughes, "Optical image quality and the cone mosaic," *Science* **231**, 499–501 (1986).
34. D. R. Williams, N. Sekiguchi, W. Haake, D. H. Brainard, and O. Packer, "The cost of trichromacy for spatial vision," in *Pigments to Perception*, B. B. Lee and A. Valberg, eds. (Plenum, New York, 1991), pp. 11–22.
35. F. Holmgren, *Über den Farbensinn* (Compt Rendu du Congrès International de Science et Médecine, Copenhagen, 1884), Vol. 1.
36. J. Krauskopf and R. Srebro, "Spectral sensitivity of color mechanisms: derivation from fluctuations of color appearance near threshold," *Science* **150**, 1477–1479 (1965).
37. A. W. Snyder, "Hyperacuity and interpolation by the visual pathways," *Vision Res.* **22**, 1219–1220 (1982).
38. R. A. Gonsalves, "Phase retrieval and diversity in adaptive optics," *Opt. Eng. (Bellingham)* **21**, 829–932 (1982).
39. R. G. Paxman, J. H. Seldin, M. G. Lofdahl, G. B. Scharmer, and C. U. Keller, "Evaluation of phase diversity techniques for solar-image restoration," *Astrophys. J.* **466**, 1087–1099 (1996).
40. S. Inoue and R. Oldenbourg, "Microscopes," in *Handbook of Optics*, M. Bass, E. W. Van Stryland, D. R. Williams, and W. L. Wolfe, eds. (McGraw-Hill, New York, 1995), pp. 17.1–17.52.
41. A. F. Fercher, K. Mengedocht, and W. Werner, "Eye-length measurement by interferometry with partially coherent light," *Opt. Lett.* **13**, 186–188 (1988).
42. D. Huang, E. A. Swanson, C. P. Lin, J. S. Schuman, W. G. Stinson, W. Chang, M. Hee, T. Flotte, K. Gregory, C. Puliafito, and J. Fujimoto, "Optical coherence tomography," *Science* **254**, 1178–1181 (1991).